Ionosphere Remote Sensing Using Closely Spaced GNSS Arrays

Jun Wang, Jade Morton, Colorado State University   William Bristow , University of Alaska Fairbanks

Summary: Our previous work has demonstrated that GPS L1 signal carrier phase fluctuations observed from a spaced receiver array can be used to estimate ionosphere irregularity horizontal drift velocities. The gist of the approach is to use a joint frequency analysis technique to generate high-resolution time varying spectrum information for the disturbed signal carrier phase. This poster has two objectives: First, expand upon the previous efforts by applying the same approach to other GNSS signals. Such an expansion allows the study of the self-consistency of the method and the observation of similarities / differences of GNSS signal diffraction patterns between irregularities structures at different physical scales; Second, look for the availability of the matching Super Dual Auroral Radar Network (SuperDARN) backscatter data when the GNSS receiver array records ionospheric scintillation events. A more adequate comparison scheme is proposed as opposed to the conventional one-beam approach. In addition, using the matching data from the two instruments, we compare the SuperDARN's LOS ionospheric irregularity drift velocity measurements against the GNSS receiver array estimations.

Methodology for Drift Velocity Estimation using Spaced GNSS Arrays

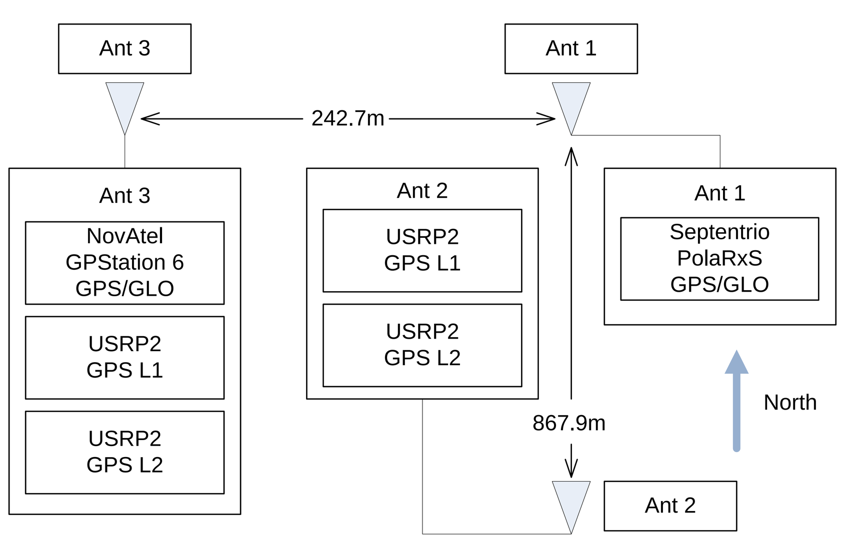

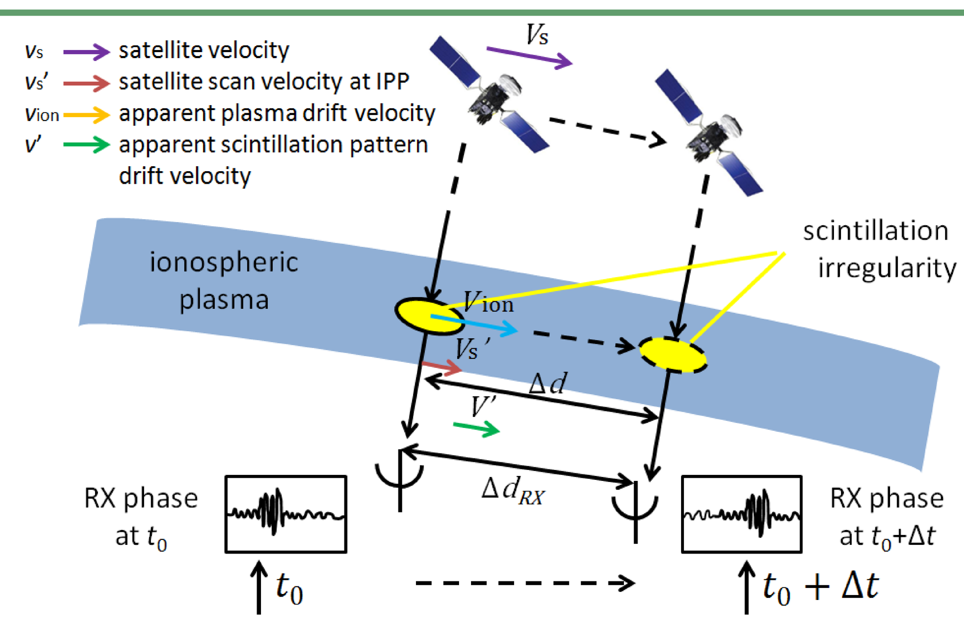

$$|v'| = \sqrt{\left(\frac{\Delta d_{1,2}}{\Delta t_{1,2}}\right)^2 + \left(\frac{\Delta d_{1,3}}{\Delta t_{1,3}}\right)^2}, \theta = \arctan\left(\frac{\Delta d_{1,2}}{\Delta t_{1,2}} \Big/ \frac{\Delta d_{1,3}}{\Delta t_{1,3}}\right)$$

$\Delta d_{i,j}$: Sub-ionospheric distance between IPP_i and IPP_j

$\Delta t_{i,j}$: Time delay between receivers i and j

Account for satellite scan velocity v_s'

$$v_{ion} = v' + v_s'$$

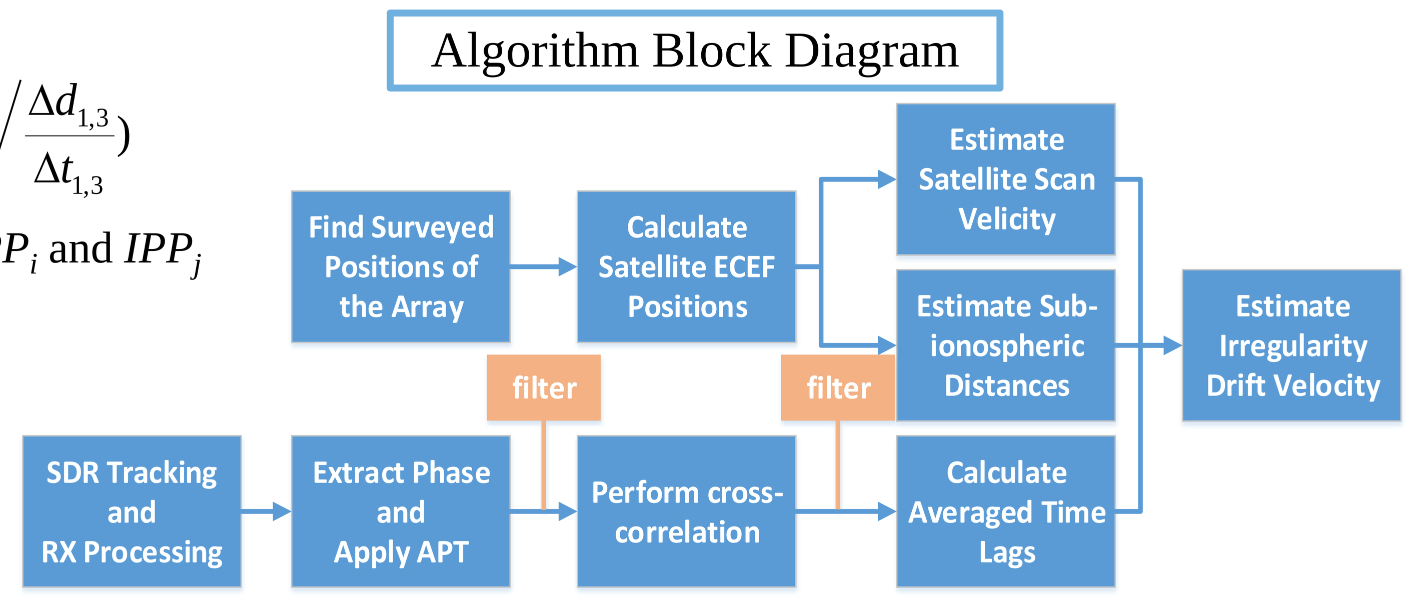

Self-Consistency Study using Multi-Band GNSS Signals

➢ Datasets used for GPS L1/L2C Study:

Date	Starting Time (UTC)	Duration (minutes)	GPS L2C (PRN)
2012/11/14	08:51:00	15	5, 7
2013/03/17	09:05:54	14	25, 29, 31
2013/03/17	10:17:10	15	5, 25, 29, 31
2013/03/17	19:08:30	28	1, 17, 31

➢ Skyplot of Estimated Drift Velocity:

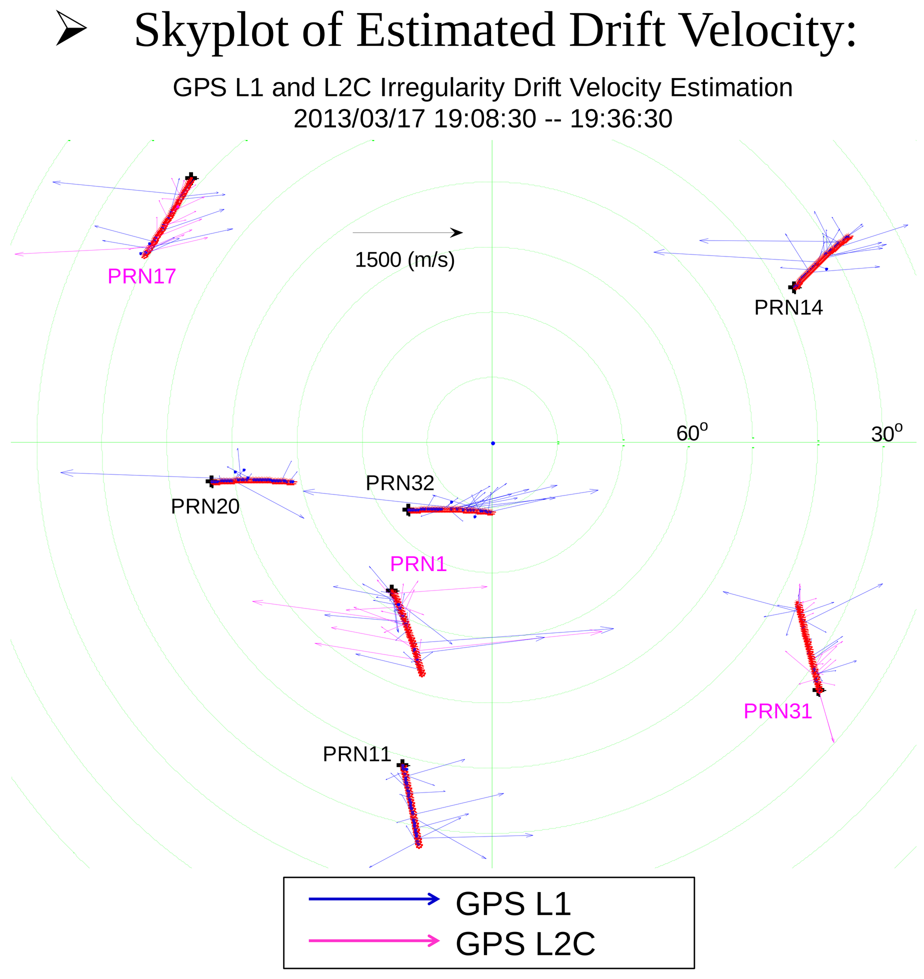

➢ Frequency Scaling: $\dfrac{\sigma_\phi(t)_{RF1}}{\sigma_\phi(t)_{RF2}} = \dfrac{f_{RF2}}{f_{RF1}}$

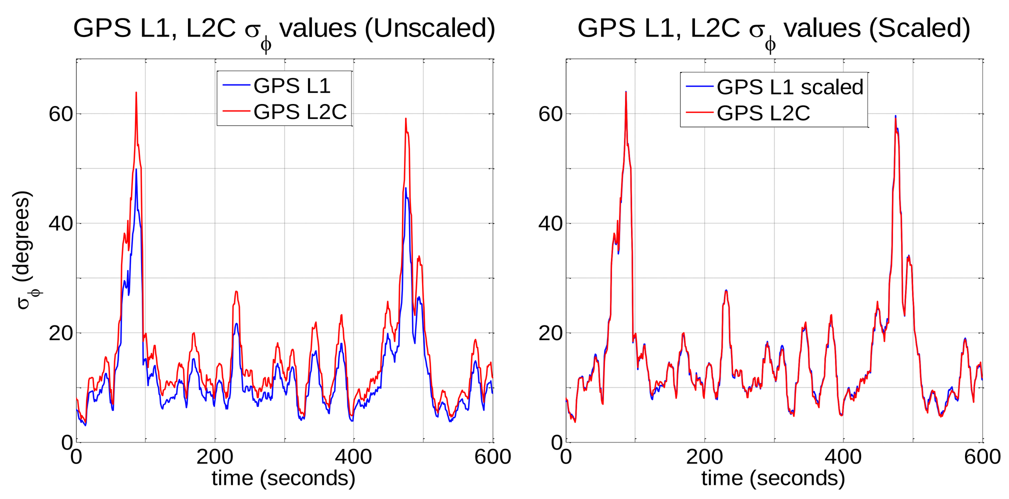

➢ Estimation Results GPS L1/L2C **combined antenna pairs** vs. **individual antenna pair**

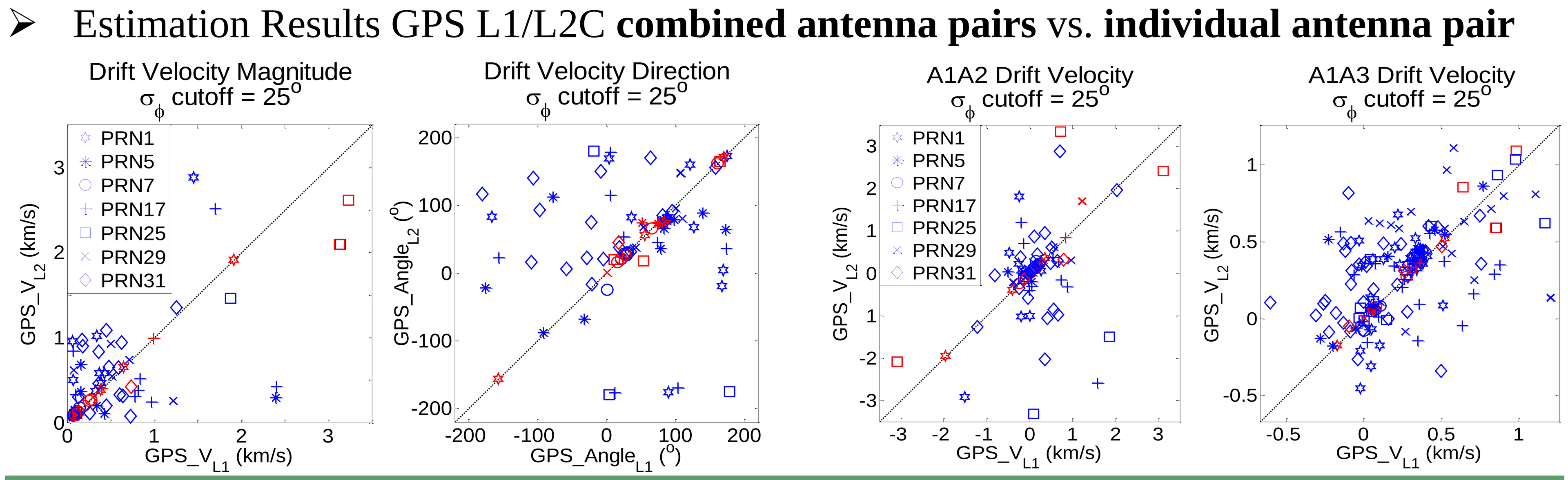

➢ Datasets used for GPS L1/L2C/L5 and GLO L1/L2 Study (A1 and A3 only):

GNSS Signal	Carrier Frequency	SV Number
GPS L2C	1575.42 MHz	1,11,14,20,32
GPS L2C	1227.60 MHz	1
GPS L5	1176.45 MHz	1
GLONASS L1	1602.0* MHz	5,6,7,15,21,22
GLONASS L2	1246.0* MHz	5,6,7,15,21,22

Date	Starting Time	Duration
2012/10/09	05:00:00 (UTC)	60 min

GLONASS carrier frequencies:

$$f_{GLONASS\_L1} = 1602.0 + n \times 0.5625\,\text{MHz}$$
$$f_{GLONASS\_L2} = 1246.0 + n \times 0.4375\,\text{MHz}$$
$$n = -7, -6, \cdots, 0, \cdots, 5, 6.$$

➢ Estimation Results GPS L1/L2C/L5 $\sigma_\phi = 15^o$ vs. $\sigma_\phi = 25^o$

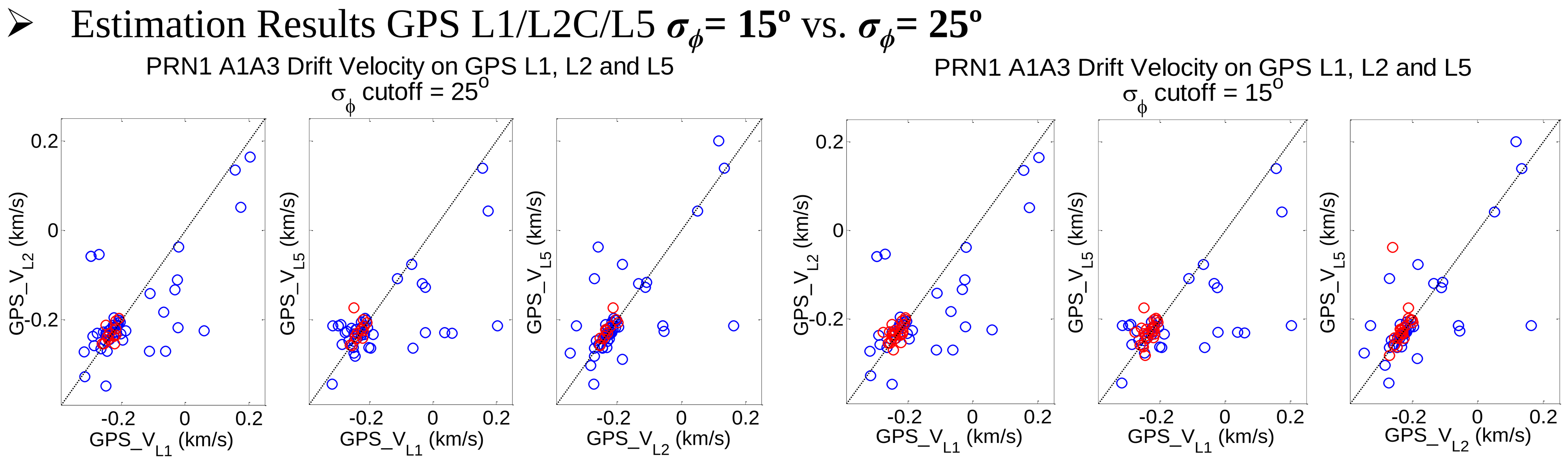

➢ Estimation Results GLO L1/L2 $\sigma_\phi = 15^o$ vs. $\sigma_\phi = 25^o$

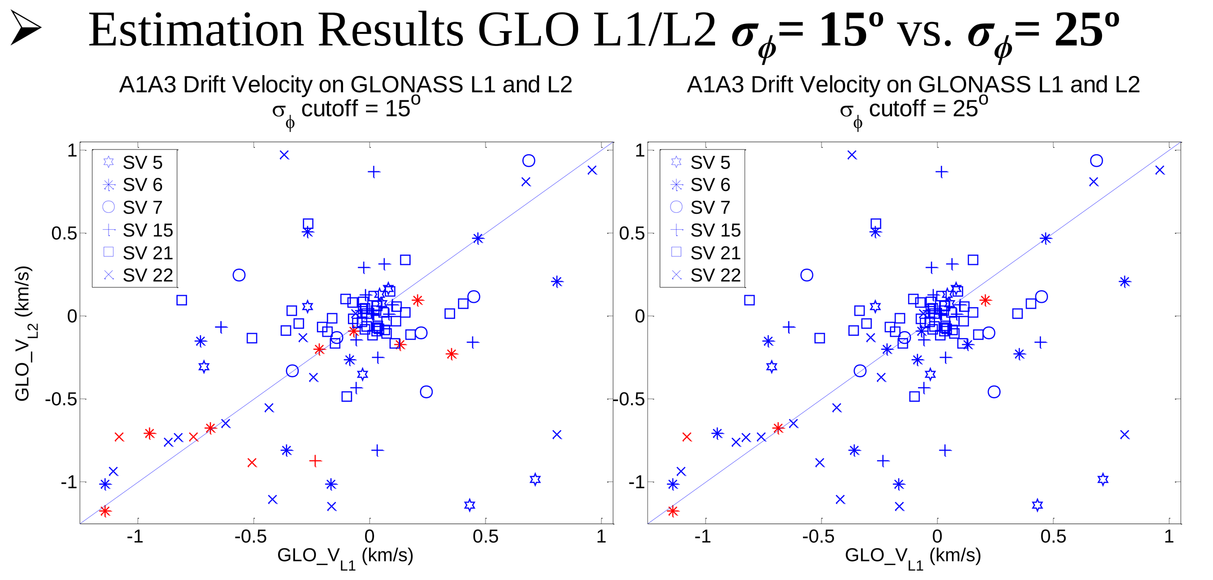

➢ Phase Noise **GPS** vs. **GLO**

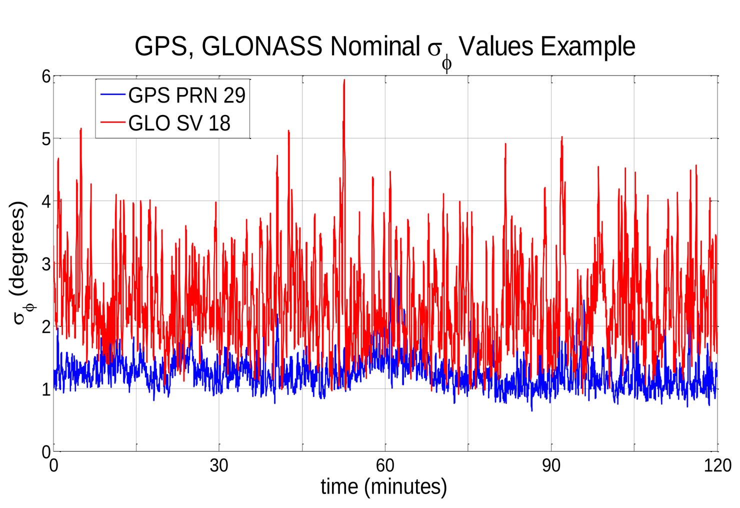

Acknowledgement

This project is funded through a grant from AFOSR (#FA9550-14-1-0265). The experimental data collection system was funded through an AFRL grant (FA8650-08-D-1451) and an AFOSR grant (FA#9550-10-1-0346). The authors would also like to acknowledge HAARP staff's support of the GNSS receiver array system setup and maintenance.

Comparative Study using GNSS Array and SuperDARN

➢ The conventional one-beam comparison schemes between GNSS receiver measurement and SuperDARN HF backscatter do not account for precise IPP locations.

➢ Problem Geometry:

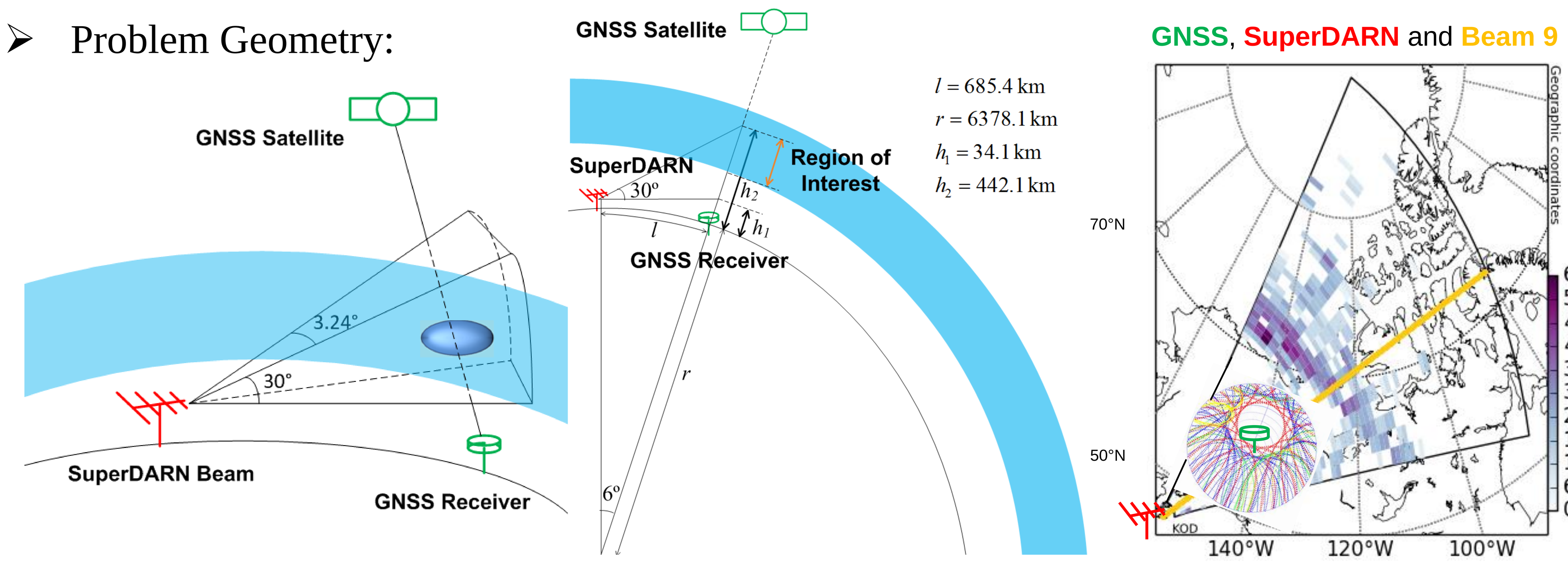

➢ Comparison method **Block Diagram** and **Algorithm**

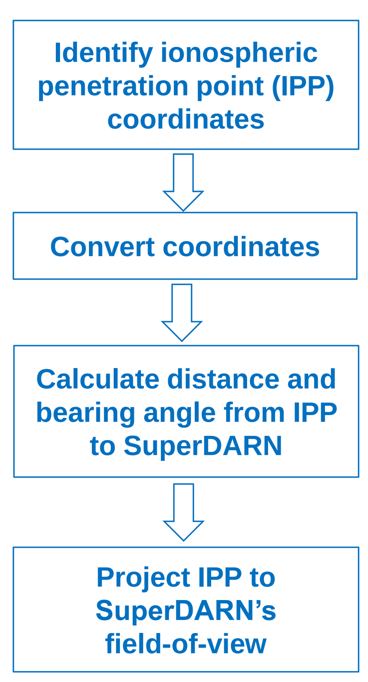

$$\angle A = 90^\circ - ele - \arcsin\left(\frac{r}{r + h_{IPP}}\cos\angle ele\right)$$
$$\varphi_{IPP} = \arcsin(\sin\varphi_{RX}\cos\angle A + \cos\varphi_{RX}\sin\angle A\cos\angle azi)$$
$$\lambda_{IPP} = \lambda_{RX} + \arcsin\left(\frac{\sin\angle A\sin\angle azi}{\cos\varphi_{IPP}}\right)$$

Geodetic → ECEF

$$d = \sqrt{(x_{IPP} - x_{SD})^2 + (y_{IPP} - y_{SD})^2 + (z_{IPP} - z_{SD})^2}$$
$$Y = \sin(\lambda_{IPP} - \lambda_{SD})\cos\varphi_{IPP}$$
$$X = \cos\varphi_{SD}\sin\varphi_{IPP} - \sin\varphi_{SD}\cos\varphi_{IPP}\cos(\lambda_{IPP} - \lambda_{SD})$$
$$\lambda_{IPP} = \arctan\left(\frac{Y}{X}\right)$$
$$x = d\sin\theta$$
$$y = d\cos\theta$$

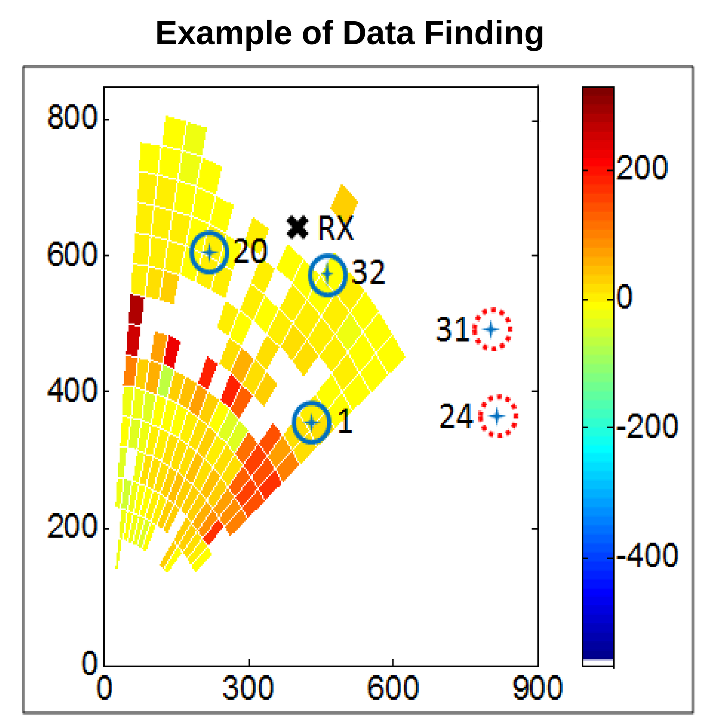

➢ SuperDARN availability (20 months) during GNSS scintillation when h_{IPP} = 350km, and h_{IPP} = [150, 450]km

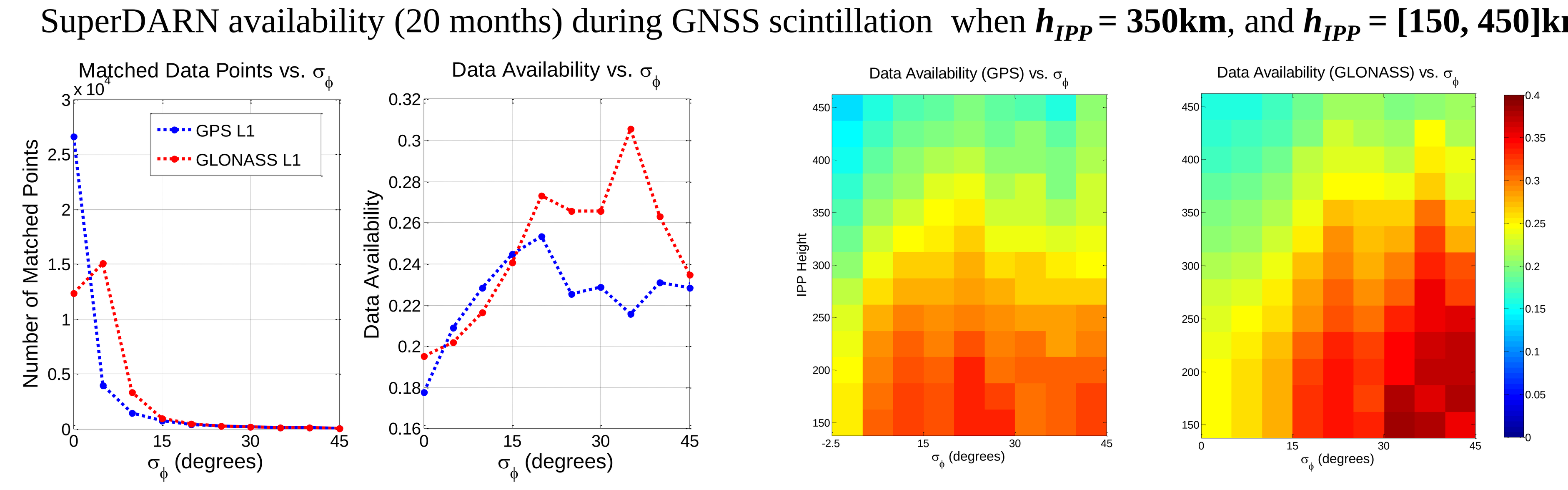

➢ **Estimated Drift Velocity** and **Comparison Results Against SuperDARN**

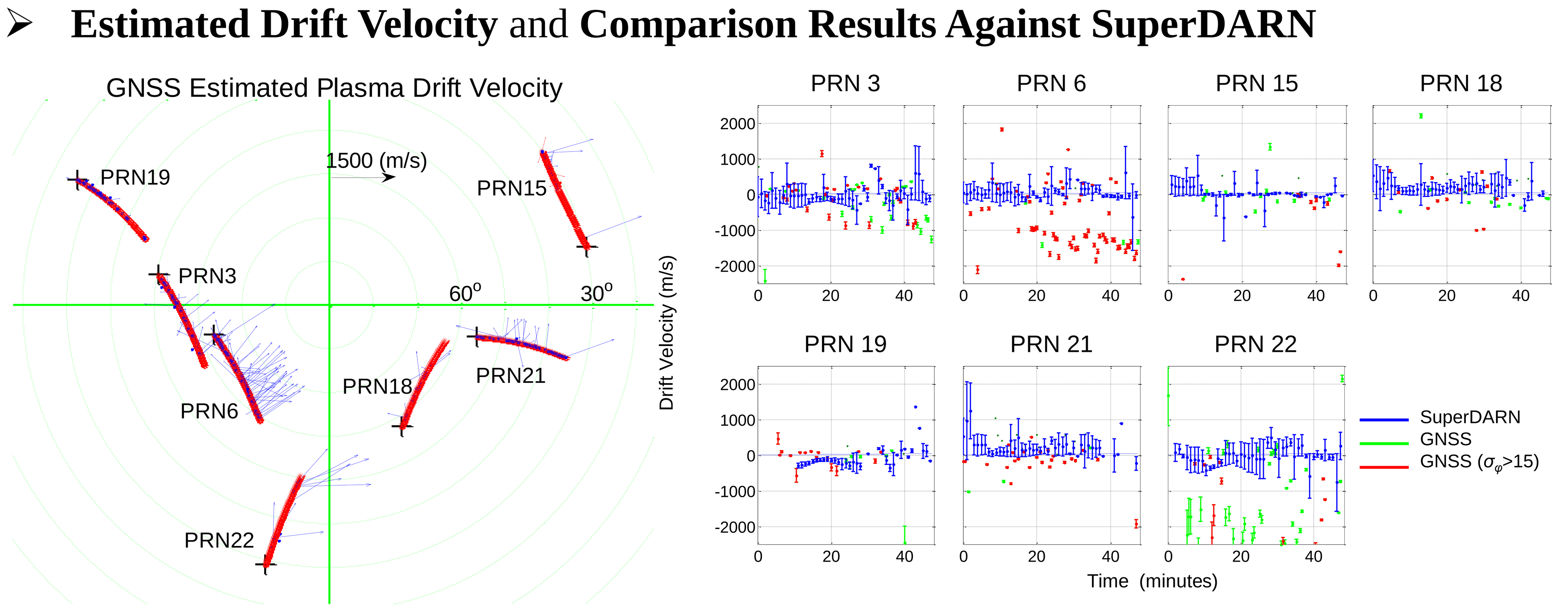

Conclusion

1. This drift velocity estimation technique together with its low cost and flexible system are especially attractive in high latitude regions, where highly dynamic phase fluctuations are more frequent and more prominent.
2. The plasma drift estimations carry high confidence level towards higher σ_ϕ threshold values.
3. The demonstrated comparison method is adequate for GNSS measurement and SuperDARN backscatter correlation studies during ionospheric scintillation. The SuperDARN data availability during scintillations maintained at a consistent level between 20% and 30% for GPS satellites, and 5% more on both ends for GLONASS satellites.
4. The GNSS estimated drift velocities do not always agree with SuperDARN measured results. SuperDARN measures the averaged behavior of the irregularities, while GNSS measures the specific behavior along the satellite-receiver LOS path.